BET bromodomain inhibition suppresses T_H17-mediated pathology

Deanna A. Mele, Andres Salmeron, Srimoyee Ghosh, Hon-Ren Huang, Barbara M. Bryant, and Jose M. Lora

Constellation Pharmaceuticals, Inc., Cambridge, MA

Interleukin (IL) 17–producing T helper (T_H17) cells have been selected through evolution for their ability to control fungal and bacterial infections. It is also firmly established that their aberrant generation and activation results in autoimmune conditions. Using a characterized potent and selective small molecule inhibitor, we show that the bromodomain and extra-terminal domain (BET) family of chromatin adaptors plays fundamental and selective roles in human and murine T_H17 differentiation from naive $CD4^+$ T cells, as well as in the activation of previously differentiated T_H17 cells. We provide evidence that BET controls T_H17 differentiation in a bromodomain-dependent manner through a mechanism that includes the direct regulation of multiple effector T_H17-associated cytokines, including *IL17*, *IL21*, and *GMCSF*. We also demonstrate that BET family members Brd2 and Brd4 associate with the *Il17* locus in T_H17 cells, and that this association requires bromodomains. We recapitulate the critical role of BET bromodomains in T_H17 differentiation in vivo and show that therapeutic dosing of the BET inhibitor is efficacious in mouse models of autoimmunity. Our results identify the BET family of proteins as a fundamental link between chromatin signaling and T_H17 biology, and support the notion of BET inhibition as a point of therapeutic intervention in autoimmune conditions.

CORRESPONDENCE
Jose M. Lora:
jose.lora@
constellationpharma.com

Abbreviations used: ChIP, chromatin immunoprecipitation; CIA, collagen-induced arthritis; EAE, experimental autoimmune encephalomyelitis; MOG, myelin oligodendrocyte glycoprotein.

The dysregulated activation and expansion of $CD4^+$ T cells lie at the core of autoimmune disorders. It is now widely recognized that T_H17 cells, a subset of T helper cells which produce IL-17A, IL-17F, IL-21, IL-22, and GM-CSF, mediate autoimmune conditions including multiple sclerosis, psoriasis, rheumatoid arthritis, and Crohn's disease, as well as the murine models of these diseases (Bettelli et al., 2006; Korn et al., 2009; Littman and Rudensky, 2010). To differentiate into T_H17 cells, naive T cells require the combined exposure to TGF-β1 and IL-6, and it is now well established that these two factors work in concert to drive the induction of a transcriptional signature that is largely orchestrated by a group of transcriptional regulators that includes steroid receptor-type nuclear receptors RORγt and RORα (Ivanov et al., 2006; Yang et al., 2008), IRF4 (IFN regulatory factor 4; Brüstle et al., 2007; Ciofani et al., 2012; Glasmacher et al., 2012), AP-1 transcription factor Batf (Schraml et al., 2009), the proto-oncogene c-Maf (Bauquet et al., 2009), NF-κB family member c-Rel (Chen et al., 2011; Ruan et al., 2011), and AHR (aryl hydrocarbon receptor; Veldhoen et al., 2008).

Global analysis of histone modifications in T cells has revealed remarkable differences in the chromatin structure of distinct T helper subsets and some of their signature transcription factors (Wei et al., 2009). Although these and other studies have begun to shed light on the role of chromatin dynamics in the control of immune lineage specification and function (Araki et al., 2009; Ramirez-Carrozzi et al., 2009), how these changes are integrated is still poorly understood. BET polypeptides BRD2, BRD3, BRD4, and BRDT harbor tandem bromodomain motifs that bind acetylated lysine residues in histones, thereby linking changes in chromatin structure with gene transcription. Indeed, BET proteins work as chromatin regulators that recruit transcriptional co-activators, such as P-TEFb, to promote gene transcription in inflammation (Hargreaves et al., 2009; Nicodeme et al., 2010) and cancer (Filippakopoulos et al., 2010; Dawson et al., 2011; Mertz et al., 2011; Zuber at al., 2011).

The Rockefeller University Press $30.00
J. Exp. Med. 2013 Vol. 210 No. 11 2181-2190
www.jem.org/cgi/doi/10.1084/jem.20130376

The Journal of Experimental Medicine

A recent report has revealed a variety of alterations in T cell cytokine production as a consequence of BET bromodomain inhibition (Bandukwala et al., 2012). However, these studies relied on transient pharmacological inhibition shortly after activation, and therefore the role of BET bromodomains during T cell subset differentiation and their potential therapeutic application remain to be defined. In this work, we provide evidence that, through bromodomain function, the BET family of chromatin adaptors play fundamental roles in T_H17 cell differentiation in vitro and in vivo, and thus represent a viable therapeutic entry point for a wide range of autoimmune disorders.

RESULTS AND DISCUSSION

BET bromodomains control human T_H17 differentiation

Because BET bromodomain inhibition results in the suppression of a subset of NF-κB–dependent genes in murine macrophages (Nicodeme et al., 2010), we hypothesized that BET proteins may also play fundamental roles in other NF-κB–mediated processes, such as T cell activation and differentiation. With that aim, we examined whether BET bromodomain inhibition had any functional impact on the differentiation of naive T cells into any major subsets (T_H1, T_H2, T_H17, and iT reg). To address this question, we used a well characterized potent and selective BET small molecule inhibitor, JQ1 (Filippakopoulos et al., 2010).

Human $CD4^+CD45RA^+$ naive T cells were purified from peripheral blood and differentiated under standard polarizing conditions in the presence of DMSO or 150 nM JQ1 (inhibitory concentration of 90% response [IC_{90}] in a THP-1 cell-based LPS-induced IL-6 release assay; unpublished data). As a control for specificity we used the inactive enantiomer of JQ1 (JQ1(−)). As shown in Fig. 1, we found a strikingly selective effect on T_H17 differentiation. After 6 d of culture, cells treated with DMSO or JQ1(−) exhibited a phenotype consistent with human T_H17 cells, as indicated by upregulation of CCR6, IL-17A, and IL-22 (Fig. 1 A). However, in the presence of JQ1, the number of $CCR6^+$ cells was severely reduced, both IL-17A and IL-22 expression were suppressed (Fig. 1 A), and the expression of RORγt (encoded by *RORC*), RORα, and a subset of T_H17 lineage-enriched transcripts were significantly inhibited (Fig. 1 C and Fig. 2 A). Under our differentiating conditions, T_H17 cells produce some IL-10, and this was also inhibited by JQ1. BET bromodomain inhibition had no effect on total cell numbers (Fig. 1 D), ruling out the possibility of T_H17 suppression as an indirect effect on T cell proliferation. JQ1 had no impact on the differentiation of T_H1 (assessed as number of IFN-γ^+ cells and *TBX21* expression), T_H2 (IL-4^+ cells and *GATA3* expression), or T reg ($FOXP3^+$ cells and *FOXP3* expression) cells (Fig. 1, B, E, and F). Thus, BET bromodomains play essential roles in the differentiation of human T_H17 cells but not other T cell lineages. The defect in T_H17 differentiation uncovered by pharmacological inhibition of BET proteins was recapitulated in siRNA experiments. Because JQ1 binds to the bromodomains of all BET family members, T cells were transfected with combinations of siRNAs targeting *BRD2* and *BRD4* (*BRD3* and *BRDT* are not expressed in T_H17 cells; unpublished data). The combined knockdown of *BRD2* and *BRD4* for 48 h resulted in significant inhibition of *RORA* and *IL17A* expression (unpublished data), confirming the data obtained with JQ1 and further ruling out a nonspecific effect of the small molecule inhibitor. Notably, BRD2 and BRD4 have nonredundant functions in T_H17 cells, as knocking down either transcript individually was sufficient to recapitulate the phenotype observed with JQ1 or with double RNA interference (Fig. 2 B). Collectively, these results highlight a critical role for BET bromodomains in promoting human T_H17 cell differentiation.

BET bromodomains are necessary for the transcription of multiple T_H17 lineage-associated cytokines, including the T_H17 autocrine amplification factor IL-21

We consistently observed a complete suppression of IL-21 transcript and protein in JQ1-treated T cells, and in fact as early as 4 h after naive T cell culture under T_H17 differentiating conditions, *Il21* was one of the top 20 transcripts most downregulated upon BET inhibition (unpublished data). IL-21 is required for the generation of T_H17 cells as an autocrine factor that induces activation of STAT3 and consequently induction of RORγt (Nurieva et al., 2007; Zhou et al., 2007). Thus, we hypothesized that BET inhibition might control T_H17 differentiation, at least in part, by directly regulating IL-21 expression. To address this possibility, we cultured human naive T cells with recombinant IL-21, and explored the impact of BET bromodomain inhibition on IL-21 mRNA expression. As previously reported (Nurieva et al., 2007; Zhou et al., 2007), exogenous IL-21 was sufficient to induce its own transcription (Fig. 2 C). This response was dependent on functional BET bromodomains, as JQ1 completely suppressed *IL21* expression (Fig. 2 C). Moreover, BET bromodomains were also essential for the background *IL21* expression observed in the absence of added IL-21 protein (Fig. 2 C, compare lanes 1 and 3). From these observations, we conclude that autocrine IL-21 expression in T cells requires functional BET bromodomains. We next determined the impact of BET inhibition on STAT3 activation and RORγt expression. Early in T_H17 differentiation, STAT3 phosphorylation is dominated by the IL-6 present in the culture medium, but over time T cell–derived IL-21 significantly contributes to this process. STAT3 activation downstream of the IL-6 receptor was not affected by BET inhibition, as JQ1 had no impact on STAT3 phosphorylation in naive cells incubated with IL-6 and TGF-β for 90 min (Fig. 2 D, top). However, BET inhibition resulted in a severe impairment of STAT3 activation and RORγt induction in cells examined after 5 d of culture under T_H17-differentiating conditions (Fig. 2, D [bottom] and F [top left]), without affecting *STAT3* expression (Fig. 2 E). Addition of exogenous IL-21 almost completely restored STAT3 activation and RORγt expression (Fig. 2, D [bottom] and F [top left]), demonstrating that by directly regulating IL-21 mRNA transcription, BET controls a fundamental amplification loop that contributes to the expression of RORγt and therefore drives optimal T_H17 differentiation.

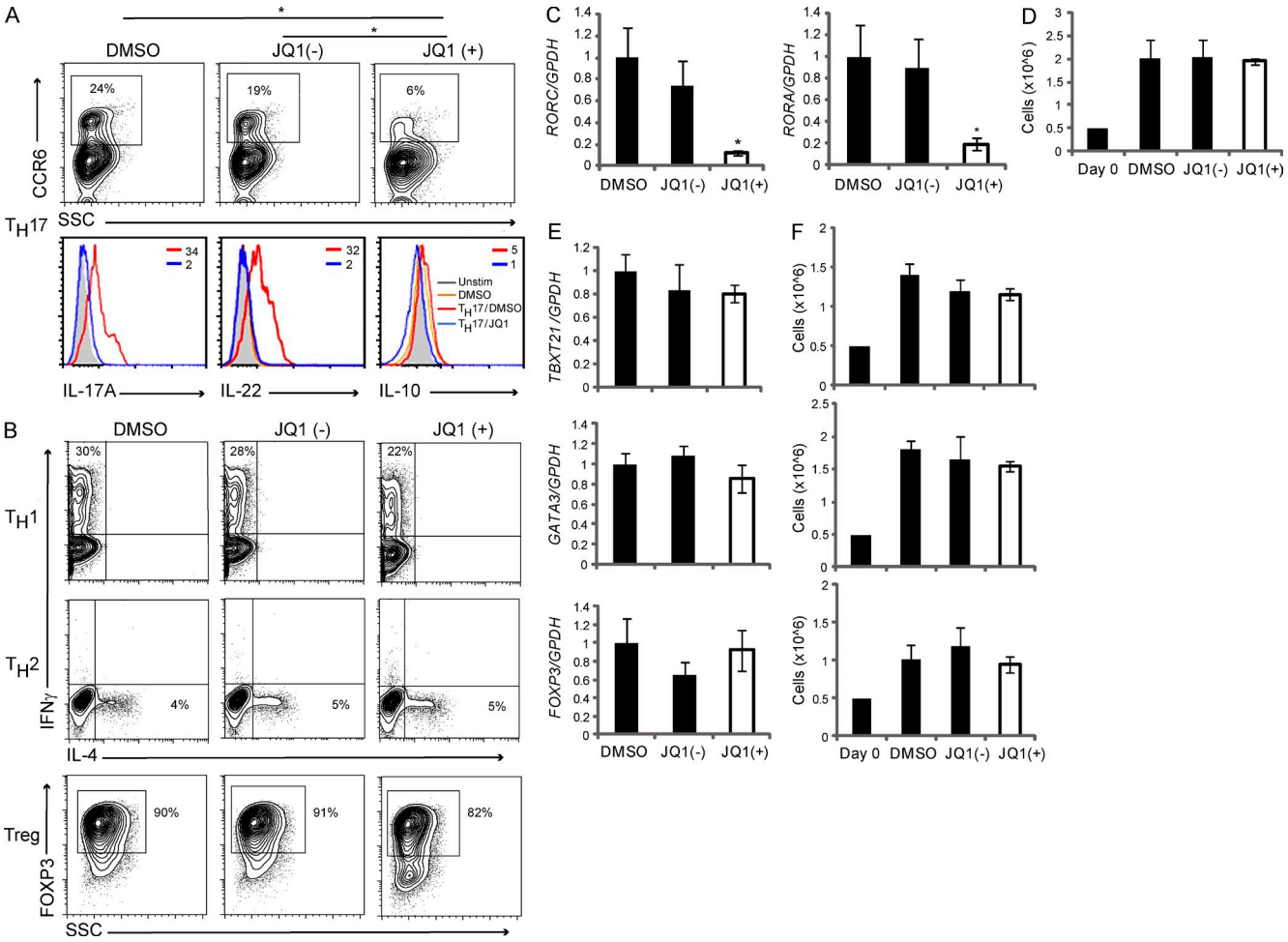

Figure 1. BET bromodomain inhibition selectively blocks human T_H17 differentiation. (A) Human CD4+CD45RA+ naive T cells were purified from peripheral blood, cultured for 6 d under T_H17 polarizing conditions with DMSO or 150 nM JQ1, and analyzed by flow cytometry. Data are representative of three to five independent experiments. Statistical significance was determined by Student *t* test, and the corresponding p-values are indicated. Percentage of IL-17–, IL-22–, and IL-10–positive cells are indicated in red (DMSO) and blue (JQ1). (B) Human naive T cells were cultured under T_H1, T_H2, and T reg polarizing conditions with DMSO or 150 nM JQ1, and analyzed by flow cytometry. Data are representative of two independent experiments. (C–F) RNA was obtained from the indicated T cell subsets and analyzed by real-time qPCR for the indicated genes at 48 h (C and E). Total cell numbers from the corresponding experiments are shown in panels D and F. Data are representative of three to five independent experiments. Error bars represent standard deviation. Statistical significance was determined by Student's *t* test (*, $P < 0.05$).

Another critical regulator of T_H17 differentiation, *BATF* (Schraml et al., 2009; Ciofani et al., 2012; Glasmacher et al., 2012), was also rescued with exogenous IL-21 (Fig. 2 F). Although the addition of IL-21 circumvented the need of BET to restore *RORC* and *BATF* expression, it did not rescue IL-17 production (Fig. 2 F), indicating that BET also directly controls the expression of IL-17. Other critical T_H17 genes, such as *GMCSF*, *IL22*, and *IL23R*, were suppressed in the presence of JQ1 and were not rescued by addition of exogenous IL-21. BET bromodomains played no role in the control of the expression of the generic proinflammatory cytokine TNF, as JQ1 did not affect its transcript levels (Fig. 2 F). Thus, BET bromodomain inhibition results in the combined and selective suppression of several key T_H17 lineage-associated genes, such as IL-17, IL-21, GM-CSF, IL-22, and IL-23R. Suppression of IL-21 results in impaired STAT3 activation, and in *RORC* and *BATF* expression. We propose that the combination of these effects of BET bromodomain inhibition results in effective suppression of T_H17 lineage differentiation.

BET bromodomain inhibition selectively suppresses the production of T_H17 cytokines in T_H17 differentiated cells

A prediction from the observed direct BET requirement for *IL17*, *IL21*, and *GMCSF* transcription is that BET bromodomain inhibition should also impair the production of those cytokines from already differentiated T_H17 cells. To address this possibility, we differentiated naive T cells under T_H17 polarizing conditions for 5 d. These newly differentiated T_H17 cells were then incubated with JQ1 and restimulated for 24 h with anti-CD3 and anti-CD28 in the absence of polarizing cytokines.

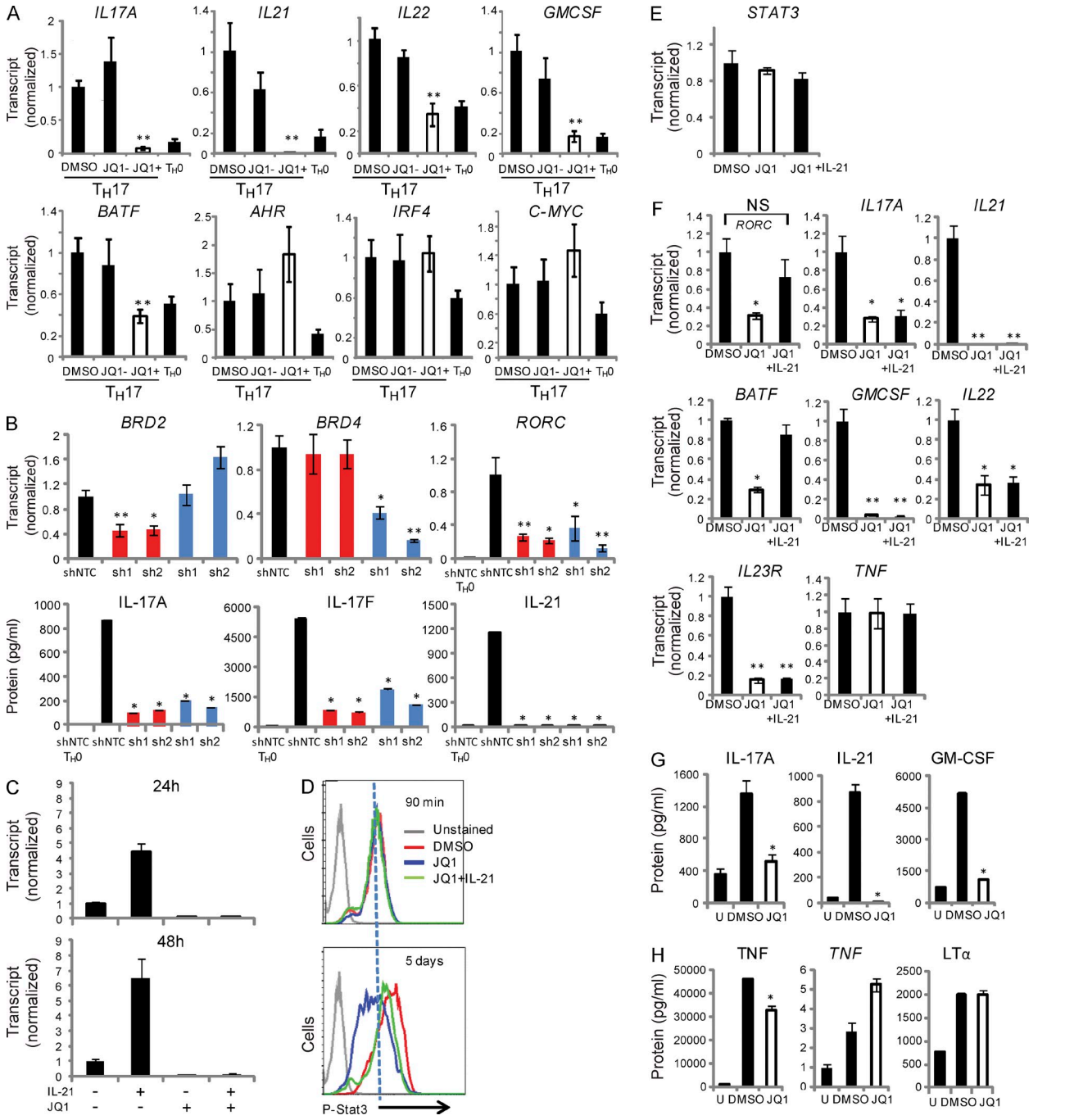

Figure 2. BET bromodomain inhibition blocks human T_H17 differentiation by controlling multiple T_H17-associated genes. (A) Human naive T cells were cultured under T_H17 conditions in the presence of 150 nM JQ1 or DMSO for 48 h and the expression of the indicated genes was investigated by qPCR. Error bars represent standard deviation. Data are representative of two to three independent experiments. Statistical significance was determined by Student's *t* test (**, $P < 0.01$). (B) Human T cells were lentivirally transduced with hairpins targeting *BRD2* (red bars) or *BRD4* (blue bars) and cultured under T_H17-polarizing conditions for 6 d. Two individual hairpins per gene were used (sh1 and sh2). Expression of *BRD2*, *BRD4*, and *RORC* was measured by qPCR; NTC, nontargeting control. IL-17A, IL-17F, and IL-21 protein was quantitated by Luminex. Data are representative of two independent experiments. Error bars represent standard deviation. Statistical significance was determined by Student's *t* test (*, $P < 0.05$; **, $P < 0.01$). (C) Human naive T cells were stimulated with anti-CD3/CD28 for 24 or 48 h in the presence or absence of exogenous human recombinant IL-21 and JQ1 as indicated, and *IL21* expression was measured by qPCR. Data are representative of two independent experiments and two independent donors. Error bars represent standard deviation. (D) Human naive T cells were cultured under T_H17-differentiating conditions for the indicated times in the presence or absence of exogenous human recombinant IL-21 and JQ1 as indicated, and phospho-Stat3 was measured by flow cytometry. Data are representative of two independent experiments and two independent donors. (E and F) Samples from D (5 d, bottom) were analyzed by qPCR for the indicated transcripts. Data are representative of two independent experiments and two independent donors. Error bars

JQ1 blocked IL-17 production in a dose-dependent manner (not depicted), approaching full suppression at a concentration of 150 nM (Fig. 2 G). In keeping with the notion of a direct role of BET in controlling multiple effector T_H17-enriched cytokines, JQ1 also abrogated IL-21 and GM-CSF production (Fig. 2 G). In contrast, the ability of these cells to produce TNF protein was only modestly ameliorated (Fig. 2 H, left) and not reduced at the transcript level (Fig. 2 H, middle). Moreover, another TNF superfamily member, lymphotoxin-α, was similarly unaffected (Fig. 2 H, right). *IL17*, *IL21*, and *GMCSF* transcripts were all reduced by JQ1 (unpublished data).

BET bromodomains control murine T_H17 differentiation

To explore if the role of BET in T_H17 differentiation has been conserved throughout evolution, and to enable pharmacological studies in mouse models of autoimmune diseases, we next sought to investigate if BET bromodomains also play critical roles in murine T_H17 cell differentiation. Naive mouse T cells were cultured under T_H17 polarizing conditions, and their phenotype upon BET inhibition was analyzed after 4 d. Early T cell activation was not affected by BET inhibition, as up-regulation of the early activation marker CD69 was unchanged (Fig. 3 A). Thus, BET bromodomains are dispensable for T cell receptor (TCR) engagement and at least some downstream signaling events. However, T_H17 differentiation was largely suppressed, as demonstrated by a significantly reduced number of IL-17A$^+$ cells determined by flow cytometry and reduced IL-17A and IL-22 secretion to the culture medium (Fig. 3 B). This suppression was not generic, as TNF was unchanged upon BET inhibition (Fig. 3 B). To further demonstrate a direct and specific effect of BET on modulating T_H17 development, we performed compound titration experiments and monitored IL-17 secretion and cell viability. IL-17 production was suppressed in a dose-dependent manner by JQ1 with an approximate IC_{50} of 30 nM, whereas cellular viability was unaffected (Fig. 3 C). From these data, we conclude that BET bromodomains are essential for mouse T_H17 differentiation.

Given the known roles of BET proteins as transcriptional co-activators, we next investigated whether BET inhibition led to changes in gene expression in T cells during T_H17 polarization. Consistent with the failure of naive T cells to differentiate into T_H17 cells in the presence of JQ1, we found the transcription of T_H17 canonical genes, such as those encoding IL-17A, IL-17F, IL-21, IL-22, IL-23R, RORα, and RORγt, to be significantly reduced by quantitative RT-PCR (qPCR) analysis (unpublished data) after 48 h of polarization. Suppression of proinflammatory gene transcription was selective, as *Tnf* remained unchanged in the presence of JQ1. Furthermore, JQ1 had no effect on the expression of *Il6r* (unpublished data), complementing the data reported above (Fig. 2 D, top) for a role of BET in T_H17 differentiation independent of early events in IL-6 signaling. These observations suggest that pharmacological blockade of BET bromodomains does not afford general gene suppression but rather a targeted effect on specific transcriptional programs. Of note, BET inhibition did not result in *c-Myc* transcript reduction (Fig. 2 A and not depicted). This observation suggests a profound cell type–specific function of BET bromodomains, as BET inhibition results in complete suppression of *c-Myc* transcription in a wide array of cancer cell lines (Dawson et al., 2011; Mertz et al., 2011; Zuber at al., 2011). Therefore, BET proteins can control nonoverlapping transcriptional programs in different cellular contexts. To extend these observations and to gain a comprehensive view of the global transcriptional changes resulting from BET inhibition in T_H17 cells, we did full-genome microarray analysis at 48 h of polarization. Strikingly, the transcriptional signature elicited by BET suppression was restricted to only 238 genes (176 down- and 62 up-regulated twofold or more; Fig. 3 D and Table S1). Highly reduced transcripts included those encoding T_H17 signature genes such as *Il17a*, *Il17f*, *Il23r*, and *Ccr6* (Fig. 3 D). Other strongly down-regulated transcripts encoded proteins that are not restricted to T_H17 cells but have been shown to be relevant for various aspects of T_H17 biology, including IL-1R1 (Chung et al., 2009). The expression patterns discussed above were confirmed by qPCR (unpublished data). As previously observed (Nicodeme et al., 2010; Mertz et al., 2011), BET inhibition also resulted in the up-regulation of a small subset of genes (Fig. 3 D and Table S1), suggesting that BET proteins can also act, directly or indirectly, as transcriptional repressors in certain genomic loci and cellular contexts. To further delineate the molecular pathways impinging upon the global transcriptional changes described above, we used the Gene Set Enrichment Analysis (GSEA) algorithm to identify curated gene signatures that significantly coincided with BET inhibition in our transcriptional profiling data. The NF-κB transcription factor target gene set scored as a highly significant overlap with the T_H17 expression set (normalized enrichment score = −1.4; P = 0.003; Fig. 3 D, bottom left). This observation is consistent with published data demonstrating a role of BET proteins in mediating NF-κB–dependent gene transcription in other cellular contexts (Hargreaves et al., 2009; Nicodeme et al., 2010). Collectively, the results reported here demonstrate that BET proteins, through their bromodomain function, play a critical role in orchestrating the transcriptional program that drives T cell differentiation into the T_H17 subset, possibly by modulating the transcriptional state of NF-κB–dependent genes. In keeping with our data from human T cells, we also observed that BET bromodomain inhibition results in a significant and dose-dependent attenuation of

represent standard deviation. Statistical significance was determined by Student's *t* test (*, P < 0.05; **, P < 0.01); NS: not significant. (G and H) Human naive T cells were cultured under T_H17 conditions for 6 d. After that time, cells were washed and rested for 16 h prior restimulation with anti-CD3/anti-CD28 for 48 h in the presence of DMSO control or 150 nM JQ1. Cytokine levels (luminex) or transcript levels (qPCR) are shown. Data are representative of two independent experiments. Error bars represent standard deviation. Statistical significance was determined by Student's *t* test (*, P < 0.05).

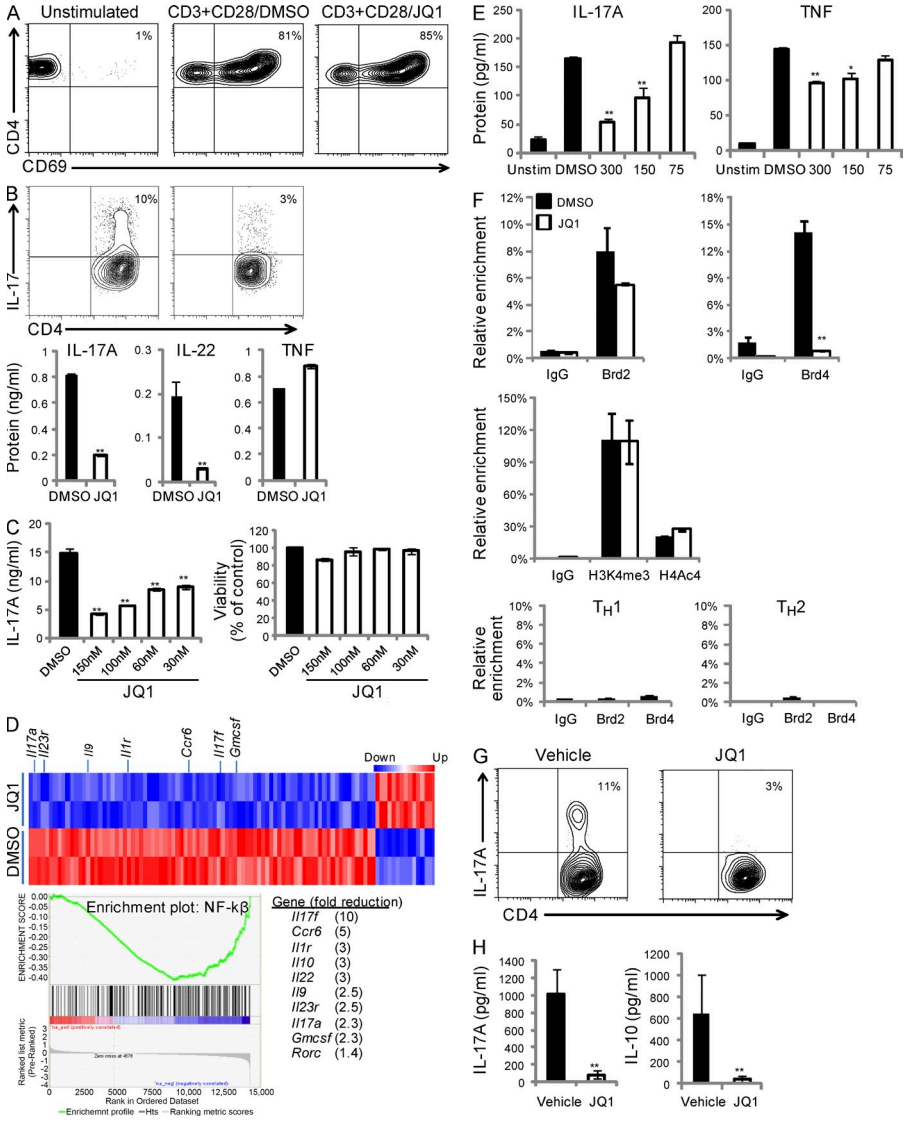

Figure 3. BET bromodomains control mouse T_H17 differentiation. (A) Mouse $CD4^+CD62L^{hi}$ naive T cells were cultured under T_H17 conditions in the presence of 150 nM JQ1 or DMSO control, and their activation state was evaluated by CD69 staining by FACS after 24 h of culture. Data are representative of three independent experiments. (B) Mouse naive T cells were cultured under T_H17 conditions in the presence of 150 nM JQ1 or DMSO control, and IL-17 induction was measured by intracellular staining (contour plots) and ELISA (bars); IL-22 and TNF were measured by ELISA (bars). Data are representative of three independent experiments. (C) JQ1 dose response inhibition was monitored by ELISA (IL-17A) and Cell Titer Glo (viability). Data are representative of three independent experiments. (D) Mouse naive T cells were cultured under T_H17 conditions in the presence of 150 nM JQ1 or DMSO control for 48 h, and whole genome gene expression was evaluated on the Affymetrix exon array platform: heatmap display, log2 expression of each gene is mean-centered, and normalized to have a standard deviation of 1; GSEA plot was calculated from the same dataset. Data represent two independent biological replicates. (E) Mouse naive T cells were differentiated into T_H17 cells for 4 d and reactivated for 18 h with anti-CD3/CD28 in the absence (filled bars) or presence (open bars) of increasing concentrations of JQ1, and IL-17A and TNF production were monitored by AlphaLISA. Data are representative of three independent experiments. (F) Brd2, Brd4, H3K4me3, and H4Ac4 ChIP was performed from naive T cells differentiated for 20 h under T_H17, T_H1, or T_H2 conditions and treated with 150 nM JQ1 or DMSO control, and examined by quantitative PCR with specific primers for the CNS2 genomic region of the *Il17* locus. IgG was used as a control. Data are representative of two to five independent experiments. (G) BET bromodomains control T_H17 differentiation in vivo. Mice were injected with anti-CD3 at times 0 and 48 h, and the duodenal T cell population was analyzed by flow cytometry 4 h after the last anti-CD3 injection in animals treated with vehicle control or 30 mg/kg JQ1 twice per day. Plasma levels of IL-17 and IL-10 were measured by ELISA (H). Data are representative of three independent experiments (n = 4–6 mice per group). All panels, error bars represent standard deviation. Statistical significance was determined by Student's t test (*, $P < 0.05$; **, $P < 0.01$).

IL-17 production in fully differentiated mouse T_H17 cells (Fig. 3 E). Although our data clearly demonstrate that BET bromodomains selectively control T_H17 differentiation, it is possible that they might modulate some biological functions of other T cell lineages, as BET inhibition results in the down-regulation of multiple genes in T_H0 cells (unpublished data).

BET members Brd2 and Brd4 directly bind to the *Il17* genomic locus in a bromodomain-dependent manner

Our observation of a requirement of functional BET bromodomains for IL-17 mRNA generation (Fig. 2, A and F) prompted us to mechanistically elucidate whether the two BET family members expressed in T_H17 cells, Brd2 and Brd4, associated with chromatin at the *Il17* locus. With that aim, we used the mouse system as a source of large number of cells to perform chromatin immunoprecipitation (ChIP) studies under T_H17 polarizing conditions. After 20 h of culture, both Brd2 and Brd4 significantly associated with chromatin at the *Il17a* control region CNS2 (essential for *Il17a* transcription; Akimzhanov et al., 2007) in T_H17 but not T_H1 or T_H2 cells, and this binding was prevented by JQ1, significantly for Brd4 (Fig. 3 F). JQ1 had no impact on H3K4me3 or acetylation on CNS2 (Fig. 3 F), suggesting that the reduced association of Brd2 and Brd4 at this site was not an indirect consequence of altered chromatin structure. Furthermore, the fact that H4Ac4 levels were unaffected (Fig. 3 F) suggests that the reduced binding of BET at CNS2 is the result of JQ1-mediated release from chromatin, and not simply an absence of the bromodomain

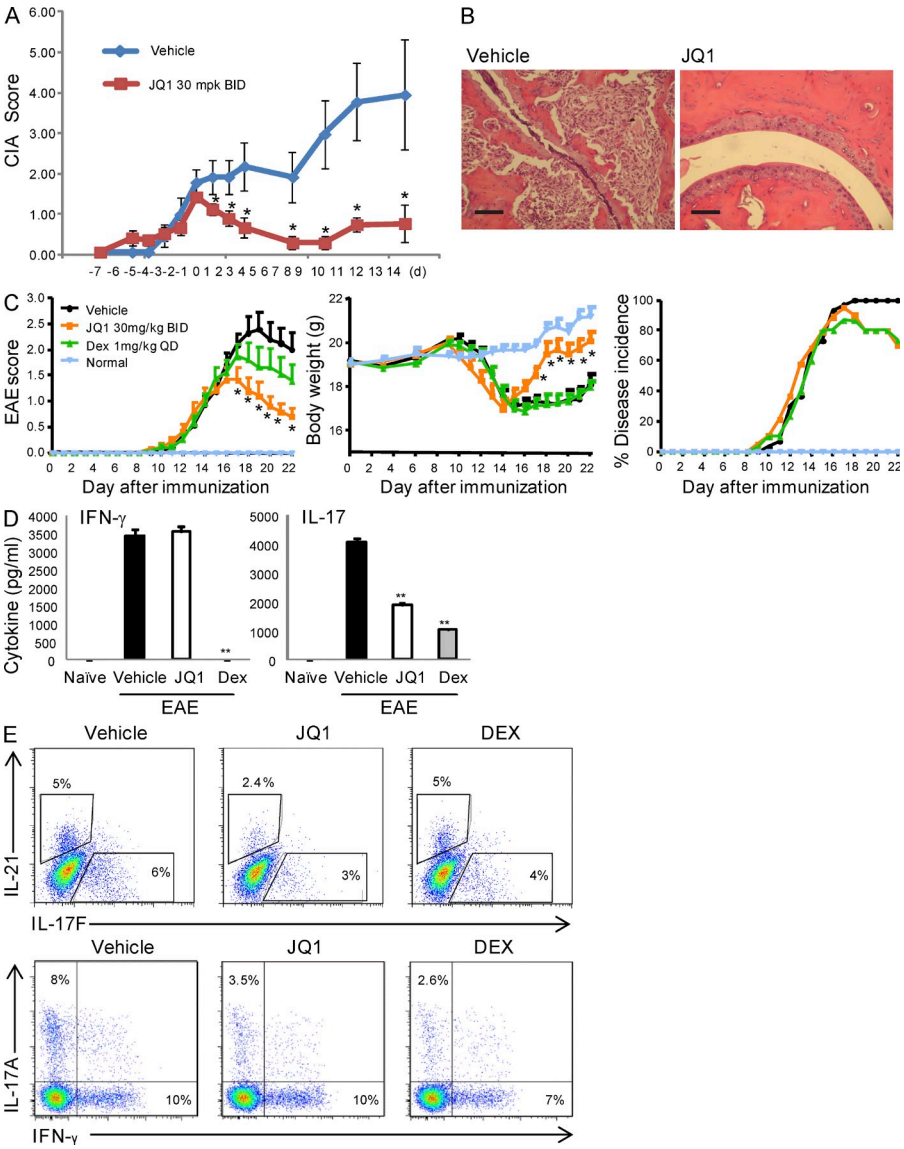

Figure 4. Inhibition of BET bromodomains protects mice from autoimmunity. (A) CIA disease progression in DBA/1 mice treated with vehicle (blue line, $n = 6$) or 30 mg/kg JQ1 (red line, $n = 14$) for 14 d. Onset of dosing is presented as day 0 in the horizontal axis. (B) Histopathology at day 14 of one representative specimen from each group. Bars, 100 µm. Data are representative of two independent experiments. Error bars represent standard deviation. *, $P < 0.05$ by Student's unpaired *t* test, two-tailed. (C) EAE disease progression in C57/B6 mice was monitored daily for changes in clinical score (left), body weight (middle), and disease incidence (right). Unimmunized animals (naive; $n = 20$) were followed in parallel. Treatment with DMSO (vehicle; $n = 30$), JQ1 (30 mg/kg; $n = 25$), or dexamethasone (Dex; $n = 30$) was started 2 wk after immunization and lasted for the remaining duration of the study. Data are representative of two independent experiments. Error bars represent standard deviation. *, $P < 0.05$ by Student's unpaired *t* test, two-tailed. (D) Single cell suspensions prepared from cervical lymph nodes of mice with EAE were restimulated with 10 µg/ml MOG peptide for 72 h and culture supernatants were assayed for the production of IFN-γ (left) and IL-17 (right) by ELISA; **, $P < 0.001$ by Student's *t* test. Error bars represent standard error of the mean. (E) Cells were isolated from the CNS of mice treated with DMSO, JQ1, or dexamethasone on day 17 after immunization with MOG peptide and stimulated ex vivo with PMA/ ionomycin, followed by intracellular cytokine staining and FACS analysis.

molecular target. Thus, BET bromodomain inhibition results in impaired binding of Brd2 and Brd4 to the *Il17a* gene and its suppressed transcription.

Inhibition of BET bromodomains blocks T_H17 differentiation in vivo

We next investigated if T_H17 suppression by BET inhibition could be recapitulated in vivo. We used a well established model where, upon two sequential injections of anti-CD3 antibody (as a way to strongly engage the TCR), an immunoregulatory environment is generated that promotes T_H17 differentiation (Esplugues et al., 2011). Consistent with previous reports demonstrating migration of T_H17 cells into the small intestine in this model, we observed a population of IL-17–producing T cells in the duodenum. Treatment of mice with the BET inhibitor resulted in a marked suppression of this duodenal T_H17 population (Fig. 3 G). In accordance with these observations, we also observed a significant reduction in the levels of circulating IL-17 in JQ1-treated animals (Fig. 3 H, left). It has been established that in this model, the duodenal T_H17 cells acquire a regulatory phenotype that includes the coexpression of *Il17* and *Il10* (Esplugues et al., 2011). Consistent with those observations, we also found a significant reduction of circulating IL-10 in the plasma of these mice upon BET inhibition (Fig. 3 H, right). It is possible that this reduction in IL-10 production is a direct transcriptional effect of BET in activated effector cells (Fig. 3 D), or a consequence of reducing the numbers of T_H17 (regulatory T_H17) cells generated in this model. Collectively, these data demonstrate a critical role for the BET bromodomains in the generation of T_H17 cells in vivo.

Inhibition of BET bromodomains protects mice from autoimmunity

The fundamental involvement of T_H17 cells in the pathogenesis of autoimmunity is firmly established. Because our data demonstrate that BET bromodomains are critical in the

differentiation and function of T_H17 cells, we hypothesized that BET inhibition could be protective in mouse models of autoimmunity. To test this hypothesis, we induced collagen-induced arthritis (CIA) and experimental autoimmune encephalomyelitis (EAE) in mice, and therapeutically used JQ1 at doses predicted to afford significant target coverage based on pharmacokinetic data (Filippakopoulos et al., 2010; unpublished data). DBA/1 mice were immunized with chicken collagen-II and left untreated until clinical signs (such as paw redness and inflammation) were observed. At that point, animals were randomly assigned to treatment with vehicle or JQ1 for 2 wk. Vehicle-treated mice continued to develop increasing clinical signs consistent with moderate-to-severe arthritis (Fig. 4 A), and histological assessment of individual joints at study termination revealed significant bone and cartilage damage, as well as extensive pannus formation (Fig. 4 B). However, mice receiving a twice-per-day (BID) dose of 30 mg/kg of the BET inhibitor were significantly protected from experimental arthritis, both macroscopically (Fig. 4 A) and histologically (Fig. 4 B). Importantly, no obvious adverse events were observed in any animal during the treatment period, as determined by monitoring body weight over the course of the experiment (unpublished data). From these data, we conclude that BET bromodomains play a pivotal role in the development and maintenance of CIA.

In a separate set of experiments, mice were immunized with a myelin oligodendrocyte glycoprotein (MOG) peptide, and when the initial signs of disease became evident (clinical score = 1) animals were treated with vehicle, JQ1, or dexamethasone (as a generic antiinflammatory control). JQ1-treated animals were significantly protected from EAE, whereas vehicle-treated animals continued to develop disease (clinical scores, body weight, and disease incidence; Fig. 4 C). To mechanistically delineate the impact of BET inhibition in this model, we isolated T cells from draining cervical lymph nodes at study termination (day 22) and reactivated them ex vivo for 3 d with MOG peptide. T cells obtained from JQ1-treated animals produced normal levels of IFN-γ but were impaired in their production of IL-17 (Fig. 4 D). At peak disease (day 17), central nervous system–infiltrating lymphocytes from vehicle-treated mice produced IL-17A, IL-17F, IL-21, and IFN-γ, whereas JQ1-treated animals showed a selective decrease in the number of cells producing IL-17A/F and IL-21, but not IFN-γ (Fig. 4 E). These results suggest that BET inhibition protects against EAE by selectively impairing the generation and/or function of T_H17 cells. Of note, T cells from dexamethasone-treated animals were impaired in the production of both IL-17A and IFN-γ (Fig. 4, D and E), with no improvement in clinical scores compared with JQ1-treated mice, highlighting the critical role of T_H17 cells in this model.

In summary, we have shown that BET proteins, through their bromodomain motifs, play critical roles in the control of T_H17 differentiation in vitro and in vivo by integrating signals that drive naive T cells into the T_H17 lineage. We have also defined a role for BET bromodomains in the selective activation of T_H17 cells once they are fully differentiated. Because T_H17 cells are essential effectors of autoimmunity, our data suggest that interfering with BET-dependent chromatin signaling may provide clinical benefit to patients suffering from this group of diseases.

MATERIALS AND METHODS

Antibodies and intracellular cytokine staining. Mouse anti-CD4 (RM4-5) and anti-CD69 (H1.2F3) were purchased from BD. Human anti-CCR6 (17–1969-42) and mouse anti-CCR6 (557976) were purchased from eBioscience and BD, respectively. For intracellular staining, cells were restimulated with 50 ng/ml PMA (Sigma-Aldrich) and 500 ng/ml ionomycin (Sigma-Aldrich) for 5 h with the addition of GolgiPlug (BD). After restimulation, the cells were washed and stained for extracellular markers, followed by fixation, permeabilization using the Cytofix/Cytoperm kit (554714; BD), and staining for intracellular cytokines to detect mouse IL-17A (559502; BD), IL-17F (561631; BD), Il-21 (12–7211-82; eBioscience), IFN-γ (554411; BD), human IL-17A (560487; eBioscience), IL-22 (12–7229-42; eBioscience), IL-10 (554707; BD), IFN-γ (17–7319; eBioscience), IL-4 (12–7049-42; eBioscience), Foxp3 (12–4777-41; eBioscience), and phoshoStat3 (557814; BD). For Foxp3 intracellular staining, cells were fixed and permeabilized using the Foxp3/Transcription Factor Staining kit (00–5523-00; eBioscience). For phospho-Stat3 intracellular staining, cells were fixed and permeabilized using Phosflow Lyse/fix Buffer (558050; BD) and Permeabilization buffer III (558049; BD). Cells were acquired on the FACSCalibur (BD) and data analyzed using FlowJo Software.

Human T cell cultures. Leukopak samples were obtained from the Biological Specialty Corporation and PBMCs were isolated by Ficoll (GE Healthcare) density gradient centrifugation. $CD4^+CD45RA^+$ T cells were isolated from PBMCs by magnetic depletion of non–T_H cells and memory $CD4^+$ T cells using the human naive $CD4^+$ T Cell Isolation kit II (130–094-131; Miltenyi Biotec). For the induction of T_H17 differentiation, naive CD4 T cells were activated using Human T-Activator CD3/CD28 Dynabeads (Invitrogen) and cultured in DMEM (Invitrogen) in the presence of the following cocktail: 2.5 ng/ml TGF-β1 (R&D Systems), 30 ng/ml IL-6 (R&D Systems), 20 ng/ml IL-23 (R&D Systems), 25 ng/ml IL-1β1 (R&D Systems), 10 μg/ml anti–human IFN-γ (clone B140; eBioscience), and 10 μg/ml anti–human IL-4 (clone 8D4-8; eBioscience) for 2–6 d. Human recombinant IL-21 was added to cell cultures when indicated at 50 ng/ml (CRI172A; Cell Sciences). For T_H1 conditions, the following cocktail was used: 10 ng/ml IL-12 (R&D Biosystems), 20 ng/ml IL-2 (R&D Biosystems), and 10 μg/ml anti–human IL-4 (clone 8D4-8; eBioscience). T_H2 conditions were 20 ng/ml IL-4 (PeproTech), 10 ng/ml IL-2 (R&D Systems), 10 μg/ml anti–human IFN-γ (clone B140; eBioscience), 20 ng/ml iT reg TGF-β1 (R&D Biosystems), and 10 ng/ml IL-2 (R&D Biosystems). Naive CD4 T cells were polarized under respective conditions for 2–6 d.

Mouse T cell cultures. Single cell suspensions of splenocytes were prepared using 70-μm nylon cell strainers (BD). Red blood cells were lysed using ammonium chloride lysis buffer (R7757; Sigma-Aldrich) and washed with cRPMI 10% FBS (61870–036; Invitrogen). Naive CD4 T cells were purified using magnetic-activated cell sorting beads (130–093-227; Miltenyi Biotec). Purity of sorted naive cells was >90%. Naive CD4 T cells from C57BL/6 mice were cultured in 24-well plates (10^6 cells/ml) and stimulated with anti-CD3/CD28–coated beads (Dynabeads 11452D; Invitrogen) for 4 d under the following T_H17 polarizing conditions: 5 ng/ml TGF-β1 (100-B; R&D Systems), 20 ng/ml IL-6 (406-ML; R&D Systems), 20 ng/ml IL-23 (1887-ML-010; R&D Systems), 10 μg/ml anti–IFN-γ antibody (554408; BD), and 10 μg/ml anti-IL-4 antibody (554432; BD). Naive CD4 T cells from C57BL/6 mice were polarized under the following T_H1 conditions: 20 ng/ml IL-12 (419-ML-010; R&D Biosystems), 10 ng/ml IL-2 (402-ML; R&D Biosystems), and 10 μg/ml anti–IL-4 antibody (554432; BD). Naive CD4 T cells from BALB/c mice were used for the following T_H2 polarizing conditions: 10 ng/ml IL-4 (214–14; PeproTech), 10 ng/ml IL-2 (402-ML; R&D Systems), and 10 μg/ml anti–IFN-γ antibody (554408; BD).

Cell viability. Cell viability was assessed using Cell Titer Glo which determines the number of viable cells based on quantification of ATP present (G7572; Promega). Live cell numbers were determined by trypan blue staining followed by analysis using Countess automated cell counter (Invitrogen).

shRNAs and lentivirus transduction of human primary T cells. Target sequences for human *BRD2* and *BRD4* were obtained from Cellecta. Sense and antisense oligonucleotides (66 nt) containing sense, loop, and antisense sequences were obtained with 5′ phosphorylation from Integrated DNA Technologies. Oligonucleotides were annealed and ligated into a lentiviral shRNA vector based on pLKO.1 obtained from Cellecta. In this vector, shRNA expression is driven by the U6 promoter, and both a fluorescence marker and puromycin acetyltransferase (separated by the T2A sequence) are driven by the UbiC promoter. Lentiviral production was performed according to publicly available protocols (http://www.broadinstitute.org/rnai/public/resources/protocols). Naive t cells were differentiated under T_H17 conditions for 16 h, followed by a spin infection for 1.5 h with lentivirus-expressing shRNAs against *BRD2*, *BRD4*, or a nontargeting control. 24 h after infection, cells were selected with 1 μg/ml of puromycin for 5 d and supernatants and cell pellets were collected for cytokine quantification and qPCR.

Cytokine assays. Cytokines were quantified from cell assays by ELISA (IL-22, TNF, and IFN-γ; eBioscience) or AlphaLISA (IL-17A and TNF; Perkin Elmer) according to the manufacturer's instructions. Plates were read on the SPECTRAmax M2 (Molecular Devices) or the EnVision 2104 Multilabel reader. Human cytokines IL-17A, IL-17F, and IL-21 were quantified from cell assays using the Milliplex MAP Human Th17 magnetic bead panel (Millipore; HTH17MAG-14K). Cytokines were quantified in plasma by MSD multi-array assays (IL-17A and IL-10; Meso Scale Discovery) according to the manufacturer's instruction. Mouse plasma was obtained by centrifugation of blood in serum separator Microtainer tubes (365956; BD) after submandibular vein puncture or cardiac puncture.

Real-time RT-PCR. RNA was purified from cells using an RNeasy Mini kit (QIAGEN) according to the manufacturer's protocol. First-strand cDNA was synthesized using SuperScript III reverse transcription. Quantitative real-time PCR was performed using FastStart Universal Probe master mix (Roche) and TaqMan probes for transcripts encoding the proteins IL-17A, IL-17F, IL-21, IL-22, IL23R, RORγt, RORα, c-Myc, TNF, IL6R, CCR6, BATF, GM-CSF, AHR, IRF4, GATA3, TBET, FOXP3, STAT3, BRD2, BRD3, and BRD4 on the Stratagene MxPro3005p. Mouse samples were normalized using GAPDH primer/probe sets (05046211001; Roche). Human samples were normalized using GAPDH primers and universal probe library probes (Roche).

Global expression profiling. Naive $CD4^+$ T cells were treated with 150 nM JQ1 or DMSO under T_H17 polarizing conditions for 48 h. Total RNA was prepared using an RNeasy kit with on-column DNase digestion according to the manufacturer's instructions. Samples were processed and hybridized on Affymetrix exon arrays, and data were acquired, at ALMAC Diagnostics. CEL files were processed with the RMA algorithm on core probe sets using the Expression Console program (Affymetrix). Duplicate log2 expression values were averaged and subtracted to obtain log fold change. For the heat maps, genes having at least twofold change and an unadjusted Student's *t* test with p-value <0.10 was selected. Profiles were normalized for each gene across both time points for the purpose of display; only the relevant time point is shown. The gene expression data are available at the Gene Expression Omnibus with accession no. GSE37270. For gene function analysis, all genes with twofold change were selected. For Gene Set Enrichment Analysis (GSEA), mouse genes were mapped to human genes using the human and mouse orthology from The Jackson Laboratory (HMD_Human5.rpt). GSEA was run with MSIGDB set c3.all.v3.0.symbols.gmt.

ChIP assays. T cells treated with DMSO or 150 nM JQ1 were cross-linked with 1% formaldehyde at a density of 2×10^6 cells/ml for 10 min at room temperature. Chromatin preparation and ChIP were performed as previously described (Mertz et al., 2011) with the following antibodies: anti-H4 tetra-acetyl (Active Motif), anti-Brd2 (Bethyl Laboratories, Inc.), anti-Brd4 (Bethyl Laboratories, Inc.), IgG (Jackson ImmunoResearch Laboratories), and H3K4me3 (Abcam). The sequences for CNS2a primers were: forward, 5′-CAGCGTGTGGTTTGGTTTAC-3′; and reverse, 5′-CTAGGTGGG-TTCCTCACTGG-3′. The enrichment was normalized to input DNA.

In vivo T cell stimulation and intestinal lymphocyte isolation. C57BL/6 mice were purchased from Charles River and kept under specific pathogen-free conditions in the animal care facility at ViviSource Laboratories, Inc. Experimental procedures were approved by ViviSource's Institutional Animal Care and Use Committee (IACUC). 8–10-wk-old C57BL/6 female mice were injected with 30 μg anti-CD3 (145 2C11) twice, 1 h after compound treatment and again 48 h later. Eight mice per group were treated with 15 mg/kg JQ1 or vehicle control by i.p. injection twice a day. Serum was collected 6 h after the first anti-CD3 injection and at the end of the study. Mice were sacrificed 4 h after the final anti-CD3 injection. Isotype control or PBS was injected as controls. The intraepithelial lymphocytes were collected as follows: small intestines were removed and Peyer's patches were dissected. The first 5 cm of the small intestine were considered as duodenum. Intestines were cut longitudinally and then cut into 1-cm strips. Tissues were washed in Hanks's buffered saline and incubated in the presence of 0.1 mM EDTA at 37°C for 20 min while stirring. The released cells were processed through a nylon wool column to enrich for T cells. The eluate was loaded onto a Percoll gradient and centrifuged. The cells between 40 and 100% Percoll were collected and used as intestinal epithelial lymphocytes.

CIA. CIA studies were performed at Biomere, Inc. and were approved by Biomere's IACUC. DBA1/ female mice were immunized by subcutaneous injection via the tail vein using purified chicken type II collagen emulsified at a 1:1 ratio (vol/vol) in CFA, and then boosted 3 wk later using chicken type II collagen emulsified at a 1:1 ratio (vol/vol) in IFA. Approximately 2 wk after the boost, animals begun to show disease signs and treatment was initiated (day 0), and it continued for 14 d.

EAE. EAE studies were performed at WuXi App Tech Ltd and were approved by WuXi's IACUC. C57BL/6 mice were randomized into four groups and immunized subcutaneously at the base of the tail with 100 μg/mouse MOG peptide (MOG_{35-55}, MEVGWYRSPFSRVVHLYRNGK) emulsified in CFA containing 5 mg/ml *Mycobacterium tuberculosis* H37Ra. On days 0 and 2 of immunization, mice were given an i.p. injection of 0.5–1 μg pertussis toxin. Animals were scored daily for clinical signs of EAE using the following criteria: 0, normal; 1, limp tail or hind limb weakness but not both; 2, limp tail and hind limb weakness; 3, partial hind limb paralysis; 4, complete hind limb paralysis; 5, moribund state or death. Treatment was initiated ∼2 wk after immunization, when the mean of clinical scores reached 1 and lasted for the remainder of the study. Mice were administered JQ1 at 30 mg/kg, i.p. twice daily, DMSO (vehicle) i.p. twice daily, and dexamethasone at 1 mg/kg orally once a day.

Chemical compound synthesis. JQ1 was synthesized according to published methods (Filippakopoulos, et al., 2010).

Online supplemental material. Table S1 shows the effect of BET bromodomains inhibition on gene expression in T_H17 cells. Online supplemental material is available at http://www.jem.org/cgi/content/full/jem.20130376/DC1.

We are grateful to Patricia Keller (Constellation Pharmaceuticals), (Pranal Dakle (Constellation Pharmaceuticals), Sara Little (ViviSource, Inc.), Drs. Stephen Dietz and Barbara Whalen (BRM, Inc.), and Dr. Shuhua Han (WuXi App Ltd) for technical assistance, and to Drs. Arthur Weiss (UCSF), Robert Sims (Constellation Pharmaceuticals), and Michael Cooper (Constellation Pharmaceuticals) for comments and critical reading of the manuscript. The authors also wish to thank Drs. Mark Goldsmith, James Audia, and Keith Dionne (Constellation Pharmaceuticals) for continuous support.

The authors are employees of Constellation Pharmaceuticals and hold stock options in Constellation Pharmaceuticals. The authors declare no further conflicts of interest.

Submitted: 19 February 2013
Accepted: 27 August 2013

REFERENCES

Akimzhanov, A.M., X.O. Yang, and C. Dong. 2007. Chromatin remodeling of interleukin-17 (IL-17)-IL-17F cytokine gene locus during inflammatory helper T cell differentiation. *J. Biol. Chem.* 282:5969–5972. http://dx.doi.org/10.1074/jbc.C600322200

Araki, Y., Z. Wang, C. Zang, W.H. Wood III, D. Schones, K. Cui, T.Y. Roh, B. Lhotsky, R.P. Wersto, W. Peng, et al. 2009. Genome-wide analysis of histone methylation reveals chromatin state-based regulation of gene transcription and function of memory $CD8^+$ T cells. *Immunity.* 30:912–925. http://dx.doi.org/10.1016/j.immuni.2009.05.006

Bandukwala, H.S., J. Gagnon, S. Togher, J.A. Greenbaum, E.D. Lamperti, N.J. Parr, A.M.H. Molesworth, N. Smithers, K. Lee, J. Witherington, et al. 2012. Selective inhibition of CD4+ T-cell cytokine production and autoimmunity by BET protein and c-Myc inhibitors. *Proc. Natl. Acad. Sci. USA.* 109:14532–14537. http://dx.doi.org/10.1073/pnas.1212264109

Bauquet, A.T., H. Jin, A.M. Paterson, M. Mitsdoerffer, I.C. Ho, A.H. Sharpe, and V.K. Kuchroo. 2009. The costimulatory molecule ICOS regulates the expression of c-Maf and IL-21 in the development of follicular T helper cells and T_H-17 cells. *Nat. Immunol.* 10:167–175. http://dx.doi.org/10.1038/ni.1690

Bettelli, E., Y. Carrier, W. Gao, T. Korn, T.B. Strom, M. Oukka, H.L. Weiner, and V.K. Kuchroo. 2006. Reciprocal developmental pathways for the generation of pathogenic effector T_H17 and regulatory T cells. *Nature.* 441:235–238. http://dx.doi.org/10.1038/nature04753

Brüstle, A., S. Heink, M. Huber, C. Rosenplänter, C. Stadelmann, P. Yu, E. Arpaia, T.W. Mak, T. Kamradt, and M. Lohoff. 2007. The development of inflammatory $T_{(H)}$-17 cells requires interferon-regulatory factor 4. *Nat. Immunol.* 8:958–966. http://dx.doi.org/10.1038/ni1500

Chen, G., K. Hardy, E. Pagler, L. Ma, S. Lee, S. Gerondakis, S. Daley, and M.F. Shannon. 2011. The NF-κB transcription factor c-Rel is required for Th17 effector cell development in experimental autoimmune encephalomyelitis. *J. Immunol.* 187:4483–4491. http://dx.doi.org/10.4049/jimmunol.1101757

Chung, Y., S.H. Chang, G.J. Martinez, X.O. Yang, R. Nurieva, H.S. Kang, L. Ma, S.S. Watowich, A.M. Jetten, Q. Tian, and C. Dong. 2009. Critical regulation of early Th17 cell differentiation by interleukin-1 signaling. *Immunity.* 30:576–587. http://dx.doi.org/10.1016/j.immuni.2009.02.007

Ciofani, M., A. Madar, C. Galan, M. Sellars, K. Mace, F. Pauli, A. Agarwal, W. Huang, C.N. Parkurst, M. Muratet, et al. 2012. A validated regulatory network for Th17 cell specification. *Cell.* 151:289–303. http://dx.doi.org/10.1016/j.cell.2012.09.016

Dawson, M.A., R.K. Prinjha, A. Dittmann, G. Giotopoulos, M. Bantscheff, W.I. Chan, S.C. Robson, C.W. Chung, C. Hopf, M.M. Savitski, et al. 2011. Inhibition of BET recruitment to chromatin as an effective treatment for MLL-fusion leukaemia. *Nature.* 478:529–533. http://dx.doi.org/10.1038/nature10509

Esplugues, E., S. Huber, N. Gagliani, A.E. Hauser, T. Town, Y.Y. Wan, W. O'Connor Jr., A. Rongvaux, N. Van Rooijen, A.M. Haberman, et al. 2011. Control of TH17 cells occurs in the small intestine. *Nature.* 475:514–518. http://dx.doi.org/10.1038/nature10228

Filippakopoulos, P., J. Qi, S. Picaud, Y. Shen, W.B. Smith, O. Fedorov, E.M. Morse, T. Keates, T.T. Hickman, I. Felletar, et al. 2010. Selective inhibition of BET bromodomains. *Nature.* 468:1067–1073. http://dx.doi.org/10.1038/nature09504

Glasmacher, E., S. Agrawal, A.B. Chang, T.L. Murphy, W. Zeng, B. Vander Lugt, A.A. Khan, M. Ciofani, C.J. Spooner, S. Rutz, et al. 2012. A genomic regulatory element that directs assembly and function of immune-specific AP-1-IRF complexes. *Science.* 338:975–980. http://dx.doi.org/10.1126/science.1228309

Hargreaves, D.C., T. Horng, and R. Medzhitov. 2009. Control of inducible gene expression by signal-dependent transcriptional elongation. *Cell.* 138:129–145. http://dx.doi.org/10.1016/j.cell.2009.05.047

Ivanov, I.I., B.S. McKenzie, L. Zhou, C.E. Tadokoro, A. Lepelley, J.J. Lafaille, D.J. Cua, and D.R. Littman. 2006. The orphan nuclear receptor RORγt directs the differentiation program of proinflammatory IL-17+ T helper cells. *Cell.* 126:1121–1133. http://dx.doi.org/10.1016/j.cell.2006.07.035

Korn, T., E. Bettelli, M. Oukka, and V.K. Kuchroo. 2009. IL-17 and Th17 cells. *Annu. Rev. Immunol.* 27:485–517. http://dx.doi.org/10.1146/annurev.immunol.021908.132710

Littman, D.R., and A.Y. Rudensky. 2010. Th17 and regulatory T cells in mediating and restraining inflammation. *Cell.* 140:845–858. http://dx.doi.org/10.1016/j.cell.2010.02.021

Mertz, J.A., A.R. Conery, B.M. Bryant, P. Sandy, S. Balasubramanian, D.A. Mele, L. Bergeron, and R.J. Sims III. 2011. Targeting MYC dependence in cancer by inhibiting BET bromodomains. *Proc. Natl. Acad. Sci. USA.* 108:16669–16674. http://dx.doi.org/10.1073/pnas.1108190108

Nicodeme, E., K.L. Jeffrey, U. Schaefer, S. Beinke, S. Dewell, C.W. Chung, R. Chandwani, I. Marazzi, P. Wilson, H. Coste, et al. 2010. Suppression of inflammation by a synthetic histone mimic. *Nature.* 468:1119–1123. http://dx.doi.org/10.1038/nature09589

Nurieva, R., X.O. Yang, G. Martinez, Y. Zhang, A.D. Panopoulos, L. Ma, K. Schluns, Q. Tian, S.S. Watowich, A.M. Jetten, and C. Dong. 2007. Essential autocrine regulation by IL-21 in the generation of inflammatory T cells. *Nature.* 448:480–483. http://dx.doi.org/10.1038/nature05969

Ramirez-Carrozzi, V.R., D. Braas, D.M. Bhatt, C.S. Cheng, C. Hong, K.R. Doty, J.C. Black, A. Hoffmann, M. Carey, and S.T. Smale. 2009. A unifying model for the selective regulation of inducible transcription by CpG islands and nucleosome remodeling. *Cell.* 138:114–128. http://dx.doi.org/10.1016/j.cell.2009.04.020

Ruan, Q., V. Kameswaran, Y. Zhang, S. Zheng, J. Sun, J. Wang, J. DeVirgiliis, H.C. Liou, A.A. Beg, and Y.H. Chen. 2011. The Th17 immune response is controlled by the Rel-RORγ-RORγ T transcriptional axis. *J. Exp. Med.* 208:2321–2333. http://dx.doi.org/10.1084/jem.20110462

Schraml, B.U., K. Hildner, W. Ise, W.L. Lee, W.A. Smith, B. Solomon, G. Sahota, J. Sim, R. Mukasa, S. Cemerski, et al. 2009. The AP-1 transcription factor *Batf* controls $T_{(H)}17$ differentiation. *Nature.* 460:405–409.

Veldhoen, M., K. Hirota, A.M. Westendorf, J. Buer, L. Dumoutier, J.C. Renauld, and B. Stockinger. 2008. The aryl hydrocarbon receptor links T_H17-cell-mediated autoimmunity to environmental toxins. *Nature.* 453:106–109. http://dx.doi.org/10.1038/nature06881

Wei, G., L. Wei, J. Zhu, C. Zang, J. Hu-Li, Z. Yao, K. Cui, Y. Kanno, T.Y. Roh, W.T. Watford, et al. 2009. Global mapping of H3K4me3 and H3K27me3 reveals specificity and plasticity in lineage fate determination of differentiating $CD4^+$ T cells. *Immunity.* 30:155–167. http://dx.doi.org/10.1016/j.immuni.2008.12.009

Yang, X.O., B.P. Pappu, R. Nurieva, A. Akimzhanov, H.S. Kang, Y. Chung, L. Ma, B. Shah, A.D. Panopoulos, K.S. Schluns, et al. 2008. T helper 17 lineage differentiation is programmed by orphan nuclear receptors ROR α and ROR γ. *Immunity.* 28:29–39. http://dx.doi.org/10.1016/j.immuni.2007.11.016

Zhou, L., I.I. Ivanov, R. Spolski, R. Min, K. Shenderov, T. Egawa, D.E. Levy, W.J. Leonard, and D.R. Littman. 2007. IL-6 programs $T_{(H)}$-17 cell differentiation by promoting sequential engagement of the IL-21 and IL-23 pathways. *Nat. Immunol.* 8:967–974. http://dx.doi.org/10.1038/ni1488

Zuber, J., J. Shi, E. Wang, A.R. Rappaport, H. Herrmann, E.A. Sison, D. Magoon, J. Qi, K. Blatt, M. Wunderlich, et al. 2011. RNAi screen identifies Brd4 as a therapeutic target in acute myeloid leukaemia. *Nature.* 478:524–528. http://dx.doi.org/10.1038/nature10334